Enhanced Skin Permeation of Naltrexone by Pulsed Electromagnetic Fields in Human Skin *In Vitro*

GAYATHRI KRISHNAN,[1] JEFFREY EDWARDS,[2] YAN CHEN,[1] HEATHER A.E. BENSON[1]

[1]Curtin Health Innovation Research Institute, School of Pharmacy, Curtin University, Perth, WA, Australia

[2]OBJ Ltd, Perth, WA, Australia

Received 29 May 2009; revised 28 September 2009; accepted 27 October 2009

Published online in Wiley InterScience (www.interscience.wiley.com). DOI 10.1002/jps.22024

ABSTRACT: The aim of the present study was to evaluate the skin permeation of naltrexone (NTX) under the influence of a pulsed electromagnetic field (PEMF). The permeation of NTX across human epidermis and a silicone membrane *in vitro* was monitored during and after application of the PEMF and compared to passive application. Enhancement ratios of NTX human epidermis permeation by PEMF over passive diffusion, calculated based on the AUC of cumulative NTX permeation to the receptor compartment verses time for 0–4 h, 4–8 h, and over the entire experiment (0–8 h) were 6.52, 5.25, and 5.66, respectively. Observation of the curve indicated an initial enhancement of NTX permeation compared to passive delivery whilst the PEMF was active (0–4 h). This was followed by a secondary phase after termination of PEMF energy (4–8 h) in which there was a steady increase in NTX permeation. No significant enhancement of NTX penetration across silicone membrane occurred with PEMF application in comparison to passively applied NTX. In a preliminary experiment PEMF enhanced the penetration of 10 nm gold nanoparticles through the stratum corneum as visualized by multi-photon microscopy. This suggests that the channels through which the nanoparticles move must be larger than the 10 nm diameter of these rigid particles.

Keywords: skin penetration enhancement; dermatology; noninvasive; inductive energy; pulsed electro magnetic field

INTRODUCTION

Naltrexone (NTX: Fig. 1) is a potent competitive opioid antagonist which has been used in several countries to assist in the maintenance of a drug-free state in the management of opioid addiction[1] and as an adjunct in the treatment of alcohol dependence.[2,3] Following conventional oral administration, NTX undergoes extensive first-pass metabolism in the liver resulting in oral bioavailability estimates in the range of 5–40%.[4,5] Adverse effects reported in oral therapy include abdominal pain, nausea, and vomiting. NTX is also capable of causing dose-related hepatocellular injury.[6] Consequently an alternative NTX delivery route that would decrease the required drug dosage could benefit the therapeutic outcome, particularly in already hepato-compromised alcohol or opioid dependent patients. Buccal delivery[7,8] with chemical and electrical enhancement and injectable sustained release depot devices[9,10] have been investigated. However the latter cannot be easily discontinued if the patient requires opiate analgesia for pain. Transdermal delivery may offer a route to circumvent the liver-related problems by allowing lower doses to be administered whilst also providing the convenience of easy discontinuation when required, however, passive delivery is not sufficient to provide therapeutic NTX levels. Stinchcomb's group have shown that lipophilic prodrugs of NTX increase the delivery rate across human skin by two- to sevenfold compared to NTX base.[11–14] More substantial NTX delivery was achieved with microneedles.[15–17]

Dermaportation is a novel transdermal drug delivery technology that uses pulsed electromagnetic fields (PEMF) to enhance the movement of substances through the skin. The technique utilizes a time varying electromagnetic field that is believed to interact with the skin to enhance transdermal delivery. At the heart of the Dermaportation system is a low-energy time varying quasi-rectangular electromagnetic (i.e., PEMF) pulse packet. Each PEMF pulse has a rapidly rising and falling edge (Fig. 2) that is hypothesized to induce localized electromagnetic field effects in the stratum corneum

Correspondence to: Heather A.E. Benson (Telephone: 618-9266-2338; Fax: 618-9266-2769; E-mail: h.benson@curtin.edu.au)

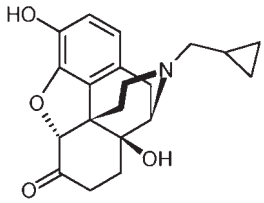

Figure 1. Chemical structure of naltrexone (NTX).

environment. The technique is noninvasive and has been demonstrated to be painless in volunteer studies.[18] In this study a local anesthetic was applied topically to the upper arms of human volunteers with the aid of PEMF over a 30 min period. Electromagnetic fields have been shown to induce changes in a number of cell types including fibroblasts, endothelial cells and keratinocytes.[19–21] It has been reported to induce wound healing[22,23] and improve chronic skin ulcers,[24,25] stimulate collagen[26] and bone growth,[27] and enhance the photodynamic effect on cancer cells.[28] We have previously demonstrated enhanced human epidermal permeation of 5-aminolevulinic acid[29] and a dipeptide[30] using the PEMF system utilized in this study. Murthy reported enhanced skin permeation of benzoic acid, salbutamol sulphate and terbutaline sulphate by magnetophoresis.[31–33] These studies involved the use of stationary permanent magnets in close proximity to the donor formulation. Murthy et al. suggested that the enhanced skin permeation observed in response to a 10 mT stationary magnet field may be due to the diffusion of the diamagnetic drug away from the magnetic field, electrosmosis or possibly altered barrier function due to the magnetic field. Electro-osmosis and increased membrane permeability have also been previously reported for increased transport of mercuric chloride and glycine through a cellulose acetate membrane under a magnetic field.[34]

A time varying magnetic field was employed in the present study. The field consisted of an asymmetrical repetition of quasi-rectangular pulses of 400 μs duration delivered at a duty cycle of 5% and a peak magnetic field of 5 mT. While the momentary peak magnetic field was consistent with Murthy et al. the average field of 0.25 mT was substantially less.

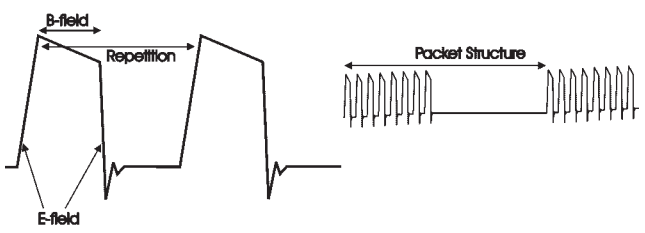

Figure 2. Schematic of a PEMF-Dermaportation waveform.

The aim of the present study was to investigate the effect of this electromagnetic energy based skin penetration enhancement technique (OBJ Dermaportation technology) on the skin penetration of NTX using an *in vitro* human epidermis diffusion model. A comparison of the effect of the PEMF on NTX permeation across human epidermis and a silicone membrane (poly-dimethylsiloxane PDMS) was incorporated to provide an insight into the mechanism of the PEMF enhanced delivery. If the PEMF energy acts primarily on the epidermal membrane there is likely to be limited NTX permeation enhancement seen with the silicone membrane but if the effect is predominately via diamagnetic repulsion or some other drug molecule-related effect enhanced permeation across silicone membrane is likely. In addition a preliminary experiment utilizing multiphoton microscopy–fluorescent lifetime imaging microscopy (MPM–FLIM) was conducted to visualize the stratum corneum penetration of 10 nm gold nanoparticles applied to human epidermis with and without PEMF.

MATERIALS AND METHODS

Materials

All the chemicals and reagents listed below were used as supplied: naltrexone hydrochloride (NTX·HCl) (>98% purity, SALARAS s.p.A, Como, Italy) was a gift from Go Medical, Perth; methanol and acetonitrile HPLC solvents from JT Baker Philipsburg, NJ; orthophosphoric acid, Ajax Finechem (Taren, Point, Australia); sodium hydroxide, analytical grade, Merck Pty Ltd. (Darmstadt, Australia). Phosphate-buffered saline solution, pH 7.4, (PBS) was prepared according to the United States Pharmacopoeia. Silicone membrane (polydimethyl siloxane membrane PDMS: "0.005" nonreinforced sheets) was obtained from Specialty Manufacturing, Inc. (Saginaw, MI). Gold nanoparticles (10 nm diameter) were obtained from the National Institute of Standards and Technology, USA.

PEMF—Dermaportation Technology

The Dermaportation technology (OBJ Ltd) used in these experiments generates an asymmetrical pulse packet type electromagnetic field comprised of a series of repeating quasi-rectangular waves of electromagnetic energy with peak maximum field strength of 5 mT. The electromagnetic pulse is propagated through the energizing of a small spirally wound monofilament air-filled coil which is placed externally to the donor compartment of a Franz type diffusion cell so that the energizing coil was 7 mm above the skin surface. The PEMF system utilizes a secure microprocessor smart card technology with automatic CRC data integrity testing and systems

 DOI 10.1002/jps

integrity testing to ensure the quality and repeatability of the field characteristics between experiments. The PEMF system used in this experiment has no user alterable controls.

HPLC System and Operations

The HPLC system (Agilent 1100) consisted of a binary pump (G1312A), 1100 thermostat autosampler (G1313A), and degasser (G1379A) equipped with 1100 photo diode array detector (G1315B). Separation of NTX·HCl was achieved on a C_{18} (150 mm × 4.6 mm) Alltech column with 5 μm particle size. Peak integration was undertaken using a personal computer equipped with Chemstation revision A 08.01 Software.

All NTX chromatographic standards were prepared by dissolving NTX·HCl in PBS (which is also used as the diffusion experiment receptor fluid), diluted with PBS and stored at 4°C until required. The mobile phase consisted of acetonitrile/water with 10 mM orthophosphoric acid (adjusted to pH 3 with sodium hydroxide) (15:85). NTX was eluted at the retention time of 4.6 min at ambient temperature at a flow rate of 1 mL/min with a 20 μL injection volume and detection wavelength of 210 nm. The assay was fully validated prior to analysis of experimental samples.

In Vitro Skin Diffusion Studies

Preparation of Membrane

Ethical approval for using human skin was obtained from the Human Research Ethics Committee of Curtin University prior to the study. Briefly, the subcutaneous tissue was removed by dissection from skin samples (abdominal region following abdominoplasty surgery at Perth Hospitals). Epidermal membranes from human skin were obtained by the heat separation method[35] where the full thickness human skin was immersed in water at 60°C for 1 min. The epidermal membrane was then teased off the dermis; placed onto aluminium foil with stratum corneum layer facing upward, air dried for 15 min and then stored at −20°C (for not more than 2 months) until required. For diffusion experiments with artificial membrane silicone membrane (polydimethyl siloxane membrane PDMS: "0.005" nonreinforced sheets) was cut in squares using scissors and soaked overnight (18 h) in MilliQ water prior to the experiment. When mounted in the Franz cells a cross sectional area of 1.18 cm^2 was available for diffusion.

In Vitro Diffusion Studies

In vitro permeation studies across human epidermis or PDMS membrane were performed using Pyrex glass Franz-type diffusion cells (enabling permeation across skin sections of cross sectional area 1.18 cm^2); receptor volume ~3.5 mL. The membrane was placed between the donor and receptor compartment of the cell and allowed to equilibrate for 1 h with PBS in the receptor compartment that was stirred continuously with a magnetic stirrer. PBS (1 mL) was placed in the donor and receptor compartments of the cell which was placed in a water bath maintained at 37 ± 0.5°C. The membrane integrity was then determined by visual inspection over a bright light and electrical resistance (kΩ), capacitance (nF), and impedance (kΩ) measurements using a digital portable LCR meter (TH2821/A/B, Changzhou Tonghui Electronic Co., Ltd, Jiangsu Province, China). TH2821B is a microprocessor-controlled portable meter with low power consumption. It was operated at 1 kHz with maximum voltage of 300 mV root-mean-square (rms) in the parallel equivalent circuit mode. The measurements were taken by immersing the stainless steel probe lead tips, one each in the donor and receptor compartments.[36] Membranes exhibiting an electrical resistance <20 kΩ were rejected from the study. The diffusion cells were emptied, receptor compartments refilled with fresh preheated PBS at 37 ± 0.5°C and 1 mL of 0.45% NTX in PBS placed in the donor compartment that was then occluded. PEMF coils were placed around the exterior of the donor compartment (Fig. 3) and energy applied for 4 h, whilst passive cells had no external PEMF energy

Figure 3. *In vitro* diffusion cell with PEMF-Dermaportation coil applied to the exterior of the cell.

applied. This was taken as time 0 and PEMF energy initiated on the active cells immediately. At different time points, aliquots from the receptor phase were withdrawn from the sampling arm and replaced with fresh preheated (at 37°C) PBS over an 8 h period. The total NTX concentration (NTX base and ions) permeating the skin into the receptor solution samples obtained from individual experiments was determined by HPLC analysis. At time 8 h the donor and receptor fluids were recovered, the cell disassembled and the skin epidermal membrane examined on a light microscope for obvious tears (any cells with torn membranes were rejected). Experiments were repeated for both the PEMF and passive applications 4 times for PDMS membrane and 13 times for human epidermal experiments. The cumulative amount of drug permeated through the epidermis and silicone membrane to the receptor compartment was plotted as a function of time. The area under the NTX cumulative permeation versus time curves (AUC) for PEMF and passive delivery was calculated (Sigma plot 8.0) and expressed as $\mu g/cm^2 h$. Enhancement ratios based on AUC were determined to compare NTX permeation in the presence of the PEMF with passive diffusion.

MPM–FLIM Analysis of Nanoparticle Penetration

A droplet of 20 μL containing a well-characterized solution of 10 nm gold nanoparticles at 51.56 ± 0.23 mg/g Au (National Institute of Standards and Technology, USA) was placed onto the stratum corneum of the human skin. The skin was exposed for 30 min prior to rinsing with 100 mL saline followed by MPM–FLIM analysis. A Dermainspect instrument with a Mai Tai laser at 740 and 850 nm was used to excite the gold nanoparticles. Second harmonic generation was quantified at lifetimes of 0–250 ps using a time-correlated photon counting module and analyzed using SPCimage software (Becker and Hickl GmbH, Berlin, Germany). Gold nanoparticle positive pixels were quantitated and graphed in untreated/unexposed and treated samples; two skin samples were treated with gold nanoparticles where one was exposed to the PEMF device and the other was not exposed to the PEMF device.

Statistical Analysis

Differences in the permeation of NTX between the PEMF and passive application were analyzed for statistical significance ($p < 0.05$) using the repeated measures ANOVA (implemented with the SAS software program using Proc Mixed). The data consist of measurements at 12 time periods on 12 samples (except that the 5 h time point was only available for 9 of the samples). Because of the skewness in the concentrations, the regression model was applied to the log-transformed data (in order to obtain the p-values for comparison of treatments). The repeated measures on each sample were taken into account, and the model essentially stated that the concentration was a function of the time delay from start and the treatment. The overall p-values were highly significant for both the treatment differences and the differences between times.

RESULTS AND DISCUSSION

In Vitro Permeation Studies of NTX Across Human Epidermis

The quantitative analysis for NTX that permeated the skin was carried out by HPLC. The samples were analyzed on a linear range 1.56–100 μg/mL with the LOD and LOQ of 134 and 449 ng/mL, respectively. The *in vitro* permeation profiles of NTX across silicone membrane and human epidermis are presented in Figures 4 and 5, respectively. The permeation parameters are given in Table 1. The data was compiled from 4 cells in silicone membrane and 13 cells in human epidermis obtained from the abdominal region of three female donors (44, 39, and 59 years). A comparison of the cumulative amount of NTX penetrating the epidermis to the receptor solution versus time was plotted for passive and PEMF applications. NTX penetration was significantly increased compared to passive application over the time period of the experiment ($p < 0.0001$). The results indicated an increase in the mean cumulative permeation of NTX over 8 h in cells where PEMF was applied, as compared to cells without PEMF application (80.2 ± 43.5, 406.9 ± 137.1 Figure 5; Tab. 1). Based on the mean cumulative permeation graph the area under the curve (AUC, Sigma Plot 8.0) was calculated (Tab. 1). PEMF energy was applied for the initial period only (0–4 h) and cumulative amount of NTX permeating to the receptor compartment during this period (mean ± SEM) was 60.6 ± 35.6 and 319.8 ±

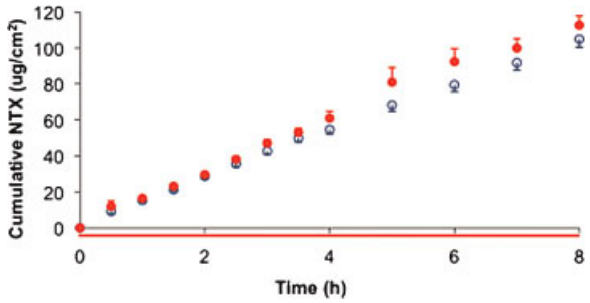

Figure 4. Cumulative amount of NTX ($\mu g/cm^2$) permeated through silicone membrane to the receptor compartment by PEMF-Dermaportation (●) and passive (○) application (mean ± SEM, $n = 4$ cells; ANOVA $p > 0.05$). PEMF applied 0–8 h.

DOI 10.1002/jps

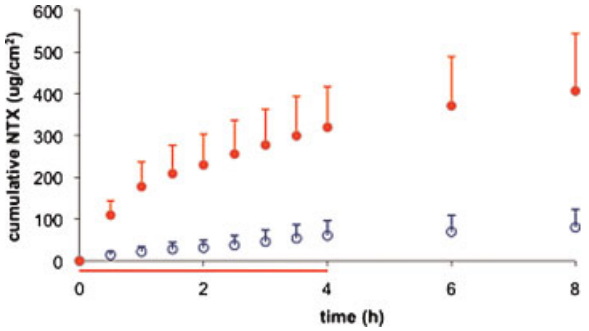

Figure 5. Cumulative amount of NTX (μg/cm^2) permeated through human epidermis to the receptor compartment by PEMF-Dermaportation (●) and passive (○) application (ANOVA $p < 0.001$). PEMF applied 0–4 h only as indicated by line on x-axis. Data represent mean ± SEM, $n = 13$ cells using skin from three human subjects.

96.7 μg/cm^2 for passive and PEMF, respectively (Tab. 1). AUC of the cumulative amount of NTX in the receptor compartment verses time graph during PEMF application (0–4 h) yielded values of 859.5 and 131.7 μg/cm^2 h for PEMF and passive, respectively, representing an enhancement ratio of 6.52. Enhancement ratios based on AUC for the entire duration of the experiment (0–8 h) and post-PEMF application (4–8 h) were 5.7 and 5.3, respectively. It is clear from observing the cumulative amount of NTX permeating human epidermis verses time profile (Fig. 5) that there is an initial PEMF enhancement effect that is maximal in the first 1.5 h of application. Post-PEMF application there is a steady increase in permeability of NTX for the remainder of the experiment.

Energy-based skin permeation enhancement of NTX has not been previously reported. However Stinchcomb's group have investigated prodrugs as a means of skin delivery.[6,11] In this case, approximately two- to sevenfold enhanced flux of lipophilic alkyl ester prodrugs compared to NTX base was achieved using NTX-3-acetate compared to NTX base in mineral oil in this experimental series.[6] These highly oil soluble prodrugs provided a higher NTX flux and underwent significant metabolic conversion in the skin. Similarly a duplex "Gemini" prodrug approach was studied where two molecules of NTX were bonded together by a carbonated ester.[14] The prodrug was hydrolyzed into two NTX moieties via skin enzymes, appearing as mainly NTX in the receptor compartment. A twofold increase in flux compared to NTX base was achieved. Transdermal delivery of NTX across microneedle-treated skin has recently been reported with clinically relevant systemic drug levels achieved in humans.[15]

In contrast to the human epidermal data, comparison of the cumulative amount of NTX penetration across silicone membrane (Fig. 4) shows only a minor difference between the PEMF and passive applications. In this study PEMF energy was applied for the entire experimental period (0–8 h) and cumulative amount of NTX permeating to the receptor compartment (mean ± SEM) was 104.9 ± 4.6 and 112.8 ± 5.1 μg/cm^2 for passive and PEMF, respectively. PDMS membranes provide a hydrophobic reproducible barrier that allows water passage equivalent to transepidermal water loss during permeation studies. This offers a simple barrier to mimic the hydrophobicity of the stratum corneum but is not subject to potential stratum corneum lipid perturbation by skin penetration enhancement techniques. For example, comparison between permeation of a solute across human skin and PDMS has been used to investigate the effects of co-solvents.[37] The comparison between the human epidermis and PDMS membrane data (Tab. 1) suggests that the mechanism of action of the PEMF may involve an interaction with the epidermal structure to provide enhanced permeation rather than a predominately drug repulsion

Table 1. Permeation Characteristics of Human Epidermal and Synthetic PDMS Membrane Under Passive and PEMF-Dermaportation Treatments

	Treatment and Time					
	0–8 h		0–4 h		4–8 h	
Parameters	P	DP	P	DP	P	DP
Human epidermis						
Mean cumulative permeation (μg/cm^2)	80.2 ± 43.4	406.9 ± 137.1	60.6 ± 35.6	319.8 ± 96.7		
Flux (μg/cm^2 h)	9.7	44.1	14.0	69.8	11.3	46.3
AUC (μg/cm^2 h)	411.7	2329.0	131.7	859.5	1469.4	280.0
Enhancement ratio (based on AUC)	5.6		6.5		5.2	
PDMS membrane						
Mean cumulative permeation (μg/cm^2)	104.9 ± 4.5	112.8 ± 5.1	54.6 ± 2.1	61.0 ± 2.2		
Flux (μg/cm^2 h)	12.9	14.2	13.6	14.7	12.2	12.4
AUC (μg/cm^2 h)	434.2	484.9	114.9	124.8	319.3	360.1
Enhancement ratio (based on AUC)	1.1		1.0		1.1	

effect as minimal enhancement was seen with the synthetic membrane.

Studies reported on the biophysical effects of other magnetic energy applications and other energy based skin permeation enhancement techniques may provide insights into the mechanism of PEMF skin permeability enhancement. There have been previous reports of the creation of cell membrane pores by magnetic particles[38] and a number of other biophysical effects of magnetic energy.[39,40] Electromagnetic waves of both high- and low-voltage pulse have been shown to perturb phospholipid layers due to electroporation and depending on the voltage and duration of pulse, molecular transport could be transcellular or intercellular. The pore size induced by electromagnetic electroporation depends on the duration and number of pulses used.[41] Typically electroporation involves higher energy, short duration pulses and therefore may not be directly relevant to PEMF effects on skin.

It could also be hypothesized that application of PEMF may increase or induce thermal transition of lipids, resulting in their restructure in the skin. During this rearrangement period the porosity of the skin may increase temporarily resulting in high permeation seen particularly during the first 1.5 h of our study with epidermal membrane (Fig. 5). Following this initial restructure a constant permeation becomes apparent which would relate to the steady NTX permeation increase post-PEMF. Silva et al.[42] showed that lipids in the stratum corneum can undergo thermal transition at temperatures below 40°C (20–40°C). However during *in vivo* studies volunteers did not report any sensation of warming of the skin due to PEMF application therefore the relevance of thermal effects may be minimal.

Movement of water molecules due to osmosis under the influence of the applied electromagnetic field could also be considered as a possible mechanism of enhancement. This mechanism has been described for iontophoresis.[43]

MPM–FLIM Analysis of Nanoparticle Penetration

Human stratum corneum/epidermis was isolated from full thickness skin by heat separation. The resulting stratum corneum/epidermis was used to assess PEMF assisted penetration of 10 nm gold nanoparticles. Initial experiments identified the major lifetime contribution of 10 nm gold nanoparticle second harmonic generation as <250 ps (Fig. 6, Panel a). This lifetime range has minimal activity ($\sim 4 \times 10^5$ pixels per 224 μm × 224 μm field of view) in untreated human skin and gold nanoparticle-treated skin without exposure to the PEMF device (Fig. 6, Panel b). Gold nanoparticle-treated human skin exposed to the PEMF device had 200 times more gold nanoparticle positive pixels than the nonexposed, but gold

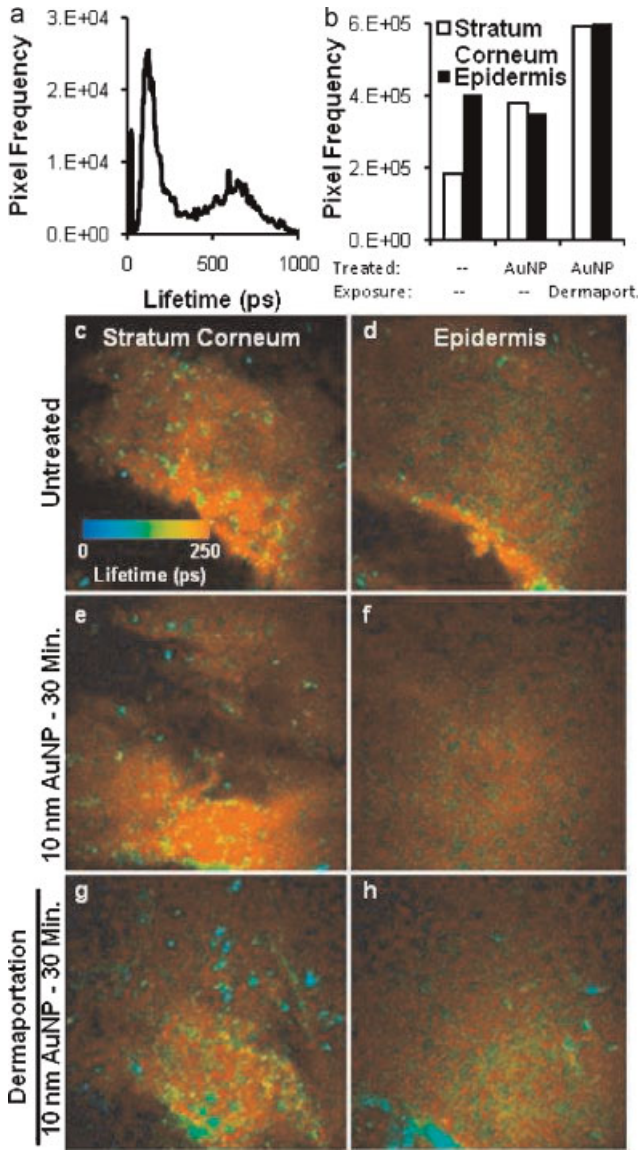

Figure 6. MPM–FLIM analysis of nanoparticle penetration enhancement by PEMF (Dermaportation). Panel a shows the lifetime profile of 10 nm gold nanoparticle second harmonic generation. The primary peak between 0 and 250 ps was used to indicate the presence of gold nanoparticles (AuNP) within the stratum corneum (white bars) and epidermis (black bars). The presence of gold nanoparticle positive pixels was quantified in both untreated (–) and treated (AuNP) human skin were analyzed by MPM–FLIM (Panel b). The treated group contained one unexposed and one PEMF-exposed (Dermaportation) piece of skin. Typical lifetime images (0–250 ps) are shown in Panels c–h and the treatment shown to the left. Panels c–h are pseudo-colored according to lifetime (bar in Panel c) where 0 is blue to 250 is red. The background levels of the stratum corneum/epidermis can be seen in Panels c and d. The major lifetime contribution of gold nanoparticle second harmonic is teal/green/yellow and can be seen particularly in the treated/PEMF-exposed samples (Panels g and h).

DOI 10.1002/jps

nanoparticle-treated group (Fig. 6, Panels b–h). The images in Panels c–h show no major differences in stratum corneum/epidermis microanatomy between the treatment groups, indicating no obvious tissue damage. This suggests that the PEMF generated magnetic field facilitates 10 nm gold nanoparticle penetration through the human stratum corneum. Furthermore, these data illustrate that the channels through which the nanoparticles move must be larger than the 10 nm diameter of these rigid particles.

CONCLUSION

Magnetic fields of both stationary and time varying type have now been shown to enhance the skin penetration of a number of solutes, including NTX, however the precise mechanism for this enhancement remains poorly understood. The difference in the level of enhancement by PEMF-Dermaportation through excised human epidermis verses silicone membrane, and the greater level of enhancement by PEMF-Dermaportation (low magnetic field strength) verses the stationary magnetic field (higher magnetic field strength), suggests that diamagnetic repulsion of a susceptible molecule is not the predominant mechanism. A potential mechanism is by interaction between the PEMF and the epidermal structure to form transient pores through which drug and water can diffuse more readily. A preliminary experiment demonstrated that PEMF enhanced the stratum corneum penetration of 10 nm particles suggesting that the channels through which the nanoparticles move must be larger than the 10 nm diameter of these rigid particles. The induction proprieties of time varying fields may play an important role in the interactions between magnetic fields and epidermal structures. Further studies are required to determine the precise mechanism of enhancement by this electromagnetic field technology.

ACKNOWLEDGMENTS

The authors are grateful for the advice and/or technical input of Dr. Jeffrey Grice, Dr. Tarl Prow, Dr. Richard Parsons, Mr. Bill Hoeneveld, Mr. Mike Boddy, Ms. Sarika Namjoshi, and Dr. Rima Cacetta. G.K. acknowledges the scholarships provided by OBJ and Curtin University (CIRTS). We also thank the surgeons and patients who provided skin for this research.

REFERENCES

1. Kirchmayer U, Davoli M, Verster AD, Amato L, Ferri A, Perucci CA. 2002. A systematic review on the efficacy of naltrexone maintenance treatment in opioid dependence. Addiction 97: 1241–1249.
2. Swift R. 2007. Emerging approaches to managing alcohol dependence. Am J Health Syst Pharm 64:S12–S22.
3. Srisurapanont M, Jarusuraisin N. 2005. Opioid antagonists for alcohol dependence. Cochrane Database Syst Rev 1: CD001867.
4. Meyer MC, Straughn AB, Lo MW, Schary WL, Whitney CC. 1984. Bioequivalence, dose-proportionality, and pharmacokinetics of naltrexone after oral administration. J Clin Psychiatr 45:15–19.
5. Gonzalez JP, Brogden RN. 1988. Naltrexone. A review of its pharmacodynamic and pharmacokinetic properties and therapeutic efficacy in the management of opioid dependence. Drugs 35:192–213.
6. Stinchcomb AL, Swaan PW, Ekabo O, Harris KK, Browe J, Hammell DC, Cooperman TA, Pearsall M. 2002. Straight-chain naltrexone ester prodrugs: Diffusion and concurrent esterase biotransformation in human skin. J Pharm Sci 91:2571–2578.
7. Giannola LI, De Caro V, Giandalia G, Siragusa MG, Tripodo C, Florena AM, Campisi G. 2007. Release of naltrexone on buccal mucosa: Permeation studies, histological aspects and matrix system design. Eur J Pharm Biopharm 67:425–433.
8. Hussain MA, Aungst BJ, Koval CA, Shefter E. 1988. Improved buccal delivery of opioid analgesics and antagonists with bitterless prodrugs. Pharm Res 5:615–618.
9. Johnson BA. 2006. A synopsis of the pharmacological rationale, properties and therapeutic effects of depot preparations of naltrexone for treating alcohol dependence. Exp Opin Pharmacother 7:1065–1073.
10. Galloway GP, Koch M, Cello R, Smith DE. 2005. Pharmacokinetics, safety, and tolerability of a depot formulation of naltrexone in alcoholics: An open-label trial. BMC Psychiatry 5:18.
11. Paudel KS, Nalluri BN, Hammell DC, Valiveti S, Kiptoo P, Hamad MO, Crooks PA, Stinchcomb AL. 2005. Transdermal delivery of naltrexone and its active metabolite 6-beta-naltrexol in human skin in vitro and guinea pigs in vivo. J Pharm Sci 94:1965–1975.
12. Nalluri BN, Milligan C, Chen J, Crooks PA, Stinchcomb AL. 2005. In vitro release studies on matrix type transdermal drug delivery systems of naltrexone and its acetyl prodrug. Drug Dev Ind Pharm 31:871–877.
13. Hammell DC, Stolarczyk EI, Klausner M, Hamad MO, Crooks PA, Stinchcomb AL. 2005. Bioconversion of naltrexone and its 3-O-alkyl-ester prodrugs in a human skin equivalent. J Pharm Sci 94:828–836.
14. Hammell DC, Hamad M, Vaddi HK, Crooks PA, Stinchcomb AL. 2004. A duplex "Gemini" prodrug of naltrexone for transdermal delivery. J Control Release 97:283–290.
15. Wermeling DP, Banks SL, Hudson DA, Gill HS, Gupta J, Prausnitz MR, Stinchcomb AL. 2008. Microneedles permit transdermal delivery of a skin-impermeant medication to humans. Proc Natl Acad Sci USA 105:2058–2063.
16. Banks SL, Pinninti RR, Gill HS, Crooks PA, Prausnitz MR, Stinchcomb AL. 2008. Flux across of microneedle-treated skin is increased by increasing charge of naltrexone and naltrexol in vitro. Pharm Res 25:1677–1685.
17. Kiptoo PK, Paudel KS, Hammell DC, Hamad MO, Crooks PA, Stinchcomb AL. 2008. In vivo evaluation of a transdermal codrug of 6-beta-naltrexol linked to hydroxybupropion in hairless guinea pigs. Eur J Pharm Sci 33:371–379.
18. Cacetta R, Eijkenboom M, Edwards J, Namjoshi S, Benson HAE. 2007. Increased transdermal delivery of local anaesthetics by the novel penetration enhancement technology Dermaportation; in vitro and in vivo assessment. Amsterdam: Pharmaceutical Sciences World Congress.

19. Bassett CA. 1989. Fundamental and practical aspects of therapeutic uses of pulsed electromagnetic fields (PEMFs). Crit Rev Biomed Eng 17:451–529.
20. Bassett CA. 1993. Beneficial effects of electromagnetic fields. J Cell Biochem 51:387–393.
21. Polk C, Postow E. 1996. Handbook of biological effects of electromagnetic fields, 9th edition. Boca Raton: CRC Press.
22. Matic M, Lazetic B, Poljacki M, Djuran V, Matic A, Gajinov Z. 2009. Influence of different types of electromagnetic fields on skin reparatory processes in experimental animals. Lasers Med Sci 24:321–327.
23. Scardino MS, Swaim SF, Sartin EA, Steiss JE, Spano JS, Hoffman CE, Coolman SL, Peppin BL. 1998. Evaluation of treatment with a pulsed electromagnetic field on wound healing, clinicopathologic variables, and central nervous system activity of dogs. Am J Vet Res 59:1177–1181.
24. Callaghan MJ, Chang EI, Seiser N, Aarabi S, Ghali S, Kinnucan ER, Simon BJ, Gurtner GC. 2008. Pulsed electromagnetic fields accelerate normal and diabetic wound healing by increasing endogenous FGF-2 release. Plast Reconstr Surg 121:130–141.
25. Milgram J, Shahar R, Levin-Harrus T, Kass P. 2004. The effect of short, high intensity magnetic field pulses on the healing of skin wounds in rats. Bioelectromagnetics 25:271–277.
26. Ahmadian S, Zarchi SR, Bolouri B. 2006. Effects of extremely-low-frequency pulsed electromagnetic fields on collagen synthesis in rat skin. Biotechnol Appl Biochem 43:71–75.
27. Colson DJ, Browett JP, Fiddian NJ, Watson B. 1988. Treatment of delayed- and non-union of fractures using pulsed electromagnetic fields. J Biomed Eng 10:301–304.
28. Pang L, Baciu C, Traitcheva N, Berg H. 2001. Photodynamic effect on cancer cells influenced by electromagnetic fields. J Photochem Photobiol B 64:21–26.
29. Namjoshi S, Cacetta R, Edwards J, Benson HAE. 2007. Liquid chromatography assay for 5-aminolevulinic acid: Application to in vitro assessment of skin penetration via Dermaportation. J Chromatogr 852:49–55.
30. Namjoshi S, Chen Y, Edwards J, Benson HA. 2008. Enhanced transdermal delivery of a dipeptide by dermaportation. Biopolymers 90:655–662.
31. Murthy SN, Hiremath SR. 2001. Physical and chemical permeation enhancers in transdermal delivery of terbutaline sulphate. AAPS PharmSciTech 2:E-TN1.
32. Murthy SN, Hiremath SR. 1999. Effect of magnetic field on the permeation of salbutamol sulphate. Indian Drugs 36:663–664.
33. Murthy SN. 1999. Magnetophoresis: An approach to enhance transdermal drug diffusion. Die Pharmazie 54:377–379.
34. Blokhra RL, Joshi J. 1999. Flow through Porous Media XVI: Electrokinetic transport coefficients of aqueous solutions of mercuric chloride and glycine through a sintered disc impregnated with a cellulose acetate membrane under a magnetic field. J Colloid Interface Sci 220:458–464.
35. Kligman A, Christophers E. 1963. Preparation of isolated sheets of human stratum corneum. Arch Dermatol 88:70–73.
36. Fasano WJ, Manning LA, Green JW. 2002. Rapid integrity assessment of rat and human epidermal membranes for in vitro dermal regulatory testing: Correlation of electrical resistance with tritiated water permeability. Toxicol In Vitro 16:731–740.
37. Megrab NA, Williams AC, Barry BA. 1995. Oestradiol permeation through human skin and silastic membrane: Effects of propylene glycol and supersaturation. J Control Release 36: 277–294.
38. Vaughan TE, Weaver JC. 1996. Energetic constraints on the creation of cell membrane pores by magnetic particles. Biophys J 71:616–622.
39. Weaver JC, Vaughan TE, Martin GT. 1999. Biological effects due to weak electric and magnetic fields: The temperature variation threshold. Biophys J 76:3026–3030.
40. Zewert TE, Pliquett UF, Vanbever R, Langer R, Weaver JC. 1999. Creation of transdermal pathways for macromolecule transport by skin electroporation and a low toxicity, pathway-enlarging molecule. Bioelectrochem Bioenerg 49: 11–20.
41. Ortega VV, Martinez AF, Gascon JY, Sanchez NA, Banos MA, Rubiales FC. 2006. Transdermal transport of India ink by electromagnetic electroporation in Guinea pigs: An ultrastructural study. Ultrastruct Pathol 30:65–74.
42. Silva CL, Nunes SC, Eusebio ME, Sousa JJ, Pais AA. 2006. Study of human stratum corneum and extracted lipids by thermomicroscopy and DSC. Chem Phys Lipids 140:36–47.
43. Delgado-Charro MB, Guy RH. 1994. Characterization of convective solvent flow during iontophoresis. Pharm Res 11:929–935.